Original Article

Evaluation of PD-L1 expression on circulating tumour cells in small-cell lung cancer

Emmanuel Acheampong[1,2]^, Afaf Abed[1,2,3], Michael Morici[1,2], Isaacs Spencer[1], Aaron B. Beasley[1,2], Samantha Bowyer[3,4,5], Du-Bois Asante[1,2], Chris Lomma[6], Weitao Lin[1,2,7], Michael Millward[1,2,3,5], Elin S. Gray[1,2]

[1]School of Medical and Health Sciences, Edith Cowan University, Joondalup, Australia; [2]Centre for Precision Health, Edith Cowan University, Joondalup, Australia; [3]Linear Clinical Research, Hospital Avenue, Nedlands, Australia; [4]Department of Medical Oncology, Sir Charles Gairdner Hospital, Hospital Avenue, Nedlands, Australia; [5]University of Western Australia, School of Medicine and Pharmacology, Crawley, Australia; [6]Department of Medical Oncology, Fiona Stanley Hospital, Murdoch, Australia; [7]Harry Perkins Institute of Medical Research, Nedlands, Australia

Contributions: (I) Conception and design: E Acheampong, ES Gray, W Lin, M Millward; (II) Administrative support: M Millward, ES Gray; (III) Provision of study materials or patients: A Abed, S Bowyer, C Lomma; (IV) Collection and assembly of data: E Acheampong, DB Asante, I Spencer, M Morici; (V) Data analysis and interpretation: E Acheampong, M Morici, W Lin, AB Beasley, ES Gray; (VI) Manuscript writing: All authors; (VII) Final approval of manuscript: All authors.

Correspondence to: Elin S. Gray. School of Medical and Health Sciences, Edith Cowan University, Joondalup 6027, Australia.
Email: e.gray@ecu.edu.au.

Background: Antibodies against the programmed death-1 (PD-1) receptor and its ligand (PD-L1) have been recently approved for small-cell lung cancer (SCLC) treatment. Circulating tumour cells (CTCs) have emerged as an appealing liquid biopsy candidate that could enhance treatment decision-making in systemic therapy for SCLC patients. Several current technologies enrich CTCs using specific surface epitopes, size, rigidity, or dielectric properties. However, they are hampered by the heterogeneity of the enriched cells from blood samples.

Methods: We evaluated two CTC enrichment systems: EpCAM conjugated to magnetic beads and a microfluidic device (Parsortix, Angle plc). PD-L1 expression was evaluated on the isolated CTCs. Twenty-three blood samples were collected from 21 patients with SCLC. PD-L1 expression was determined on CTCs through immunofluorescent staining.

Results: CTCs were found in 14/23 (60.9%) of the samples, with 11/23 (47.8%) through EpCAM-coated magnetic beads (range, 4–1,611 CTCs/8 mL; median =5) and 10/20 (50.0%) using the Parsortix system (range, 1–165 CTCs/8 mL; median =4). Notably, a total of 17 EpCAM-negative CTCs were isolated using the Parsortix system. PD-L1 expression was detected on 257 of the 3,501 (7.3%) CTCs isolated with EpCAM-coated beads and in 30/363 (8.3%) of the CTCs isolated with the Parsortix system. No vimentin expression was observed in any of the detected CTCs.

Conclusions: Overall, we identified a population of EpCAM-negative SCLC CTCs and showed that PD-L1 expression can be assessed on CTCs from SCLC patients. Comparison to tumour and treatment outcomes is needed to validate the potential of CTCs as an alternative sample for the assessment of PD-L1 expression in SCLC.

Keywords: Circulating tumours cells; PD-L1 expression; small-cell lung cancer (SCLC)

Submitted Oct 06, 2021. Accepted for publication Jan 11, 2022. This article was updated on May 06, 2022. The original version is available at: http://dx.doi.org/10.21037/tlcr-21-819.
doi: 10.21037/tlcr-21-819

^ ORCID: 0000-0002-5338-3258.

Introduction

Small-cell lung cancer (SCLC) is a highly aggressive subtype of lung cancer that accounts for approximately 15% of all lung cancers (1). It is characterised by rapid cellular proliferation and early extensive metastases (2). About 60% of patients have an extensive-stage disease at the time of diagnosis (3). Despite extensive studies, limited therapeutic advances have done little to improve SCLC patients' outcomes.

Chemotherapy and/or radiotherapy remain the principal treatment modalities for SCLC patients, who often show a high response to treatment early on (4-6). However, recurrence occurs in most cases, resulting in a poor prognosis. The 5-year overall survival (OS) rate for early-stage disease is around 15–27%, and for metastatic disease, it is reduced to ~2.8% (4-7). The use of monoclonal antibodies to block the interaction between programmed death-1 (PD-1) and its ligand (PD-L1) has appeared recently as a treatment option in non-small cell lung cancer (NSCLC), and more recently, SCLC (8,9). Expression of PD-L1 by tumour cells allows them to escape immune effector mechanisms (10). Recently, the anti-PD-L1 agents atezolizumab and durvalumab in combination with chemotherapy gained US Federal Drug Administration (FDA) approval as a first-line treatment for extensive-stage SCLC. Despite immune checkpoint inhibitors (ICIs) becoming a primary component of SCLC treatment, their efficacy is modest, with only 2 months of OS benefits and limited to a small subset of patients (8,9,11). Hence, there is a need to identify biomarkers that will help determine a subgroup of SCLC patients most likely to benefit from these treatments.

Generally, expression of PD-L1 is assessed on fine-needle aspiration biopsy or core needle biopsy tissue specimen. However, acquisition of tumour tissue is both laborious and invasive for patients. In metastatic SCLC, surgical resection and repeat tumour biopsies are not standard of care and consequently, there can be insufficient tissue for clinical analysis (12,13). Circulating tumour cells (CTCs) offer an appealing liquid biopsy modality for SCLC due to their abundance in the blood of these patients. CTCs can serve as a minimally invasive and serially acquirable substitute for tumour biopsies for tumour characterisation and evaluation of PD-L1 expression in SCLC (14,15).

CTCs are malignant cells shed into the blood by both primary and metastatic solid tumours and their presence in circulation represents a critical step in the metastatic process (16,17). CTCs can reflect the heterogeneity of SCLC tumours because they arise from different tumour sites (18,19). SCLC is distinguished by exceedingly high but variable numbers of CTCs ranging from single to thousands of CTCs per 7.5 mL of peripheral blood compared with other solid malignancies (20). The number of CTCs present are prognostic and reflect the changing disease burden throughout treatments (21,22). Yet, detection of CTCs after isolation is a challenge due to tumoural heterogeneity. Different well-established approaches to isolate and identify SCLC CTCs with different definitions of tumour cells have been published with detection rates ranging from 60% to 96% (23-25).

CellSearch, an EpCAM-based system, remains the only FDA-approved system and the most used SCLC CTC isolation platform in the clinical setting (26). With the CellSearch platform, CTCs are detectable in most SCLC patients due to the abundance of high EpCAM expressing CTCs (20-22). However, some CTCs might not express EpCAM or might have downregulated EpCAM and therefore remain undetectable with this method. To overcome the above limitation, alternative strategies based on the biophysical properties of the cells other than EpCAM protein expression are necessary (27). Such non-marker-based strategies may allow for broader coverage of CTCs subpopulations. Currently, there are several developed size-based platforms (28). Amongst them, the Parsortix system, which isolates cells based on a combination of size and deformability, has been shown to isolate CTCs where CellSearch was unable to (29).

The assessment of PD-L1 on CTCs (PD-L1$^+$ CTCs) has been extensively studied in NSCLC (30) but to our knowledge, no exhaustive report exists for SCLC. We, therefore, developed an EpCAM targeting magnetic bead-based CTC isolation method as a surrogate for CellSearch, the gold standard for CTC enumeration. Using our immunomagnetic isolation technique, we compared detection rates of CTCs isolated using EpCAM-based immunomagnetic capture to those isolated using the Parsortix system. Secondly, we established a workflow to determine the prevalence of PD-L1$^+$ CTCs in SCLC utilising EpCAM-coated magnetic beads and the Parsortix system. We present the following article in accordance with the MDAR reporting checklist (available at https://tlcr.amegroups.com/article/view/10.21037/tlcr-21-819/rc).

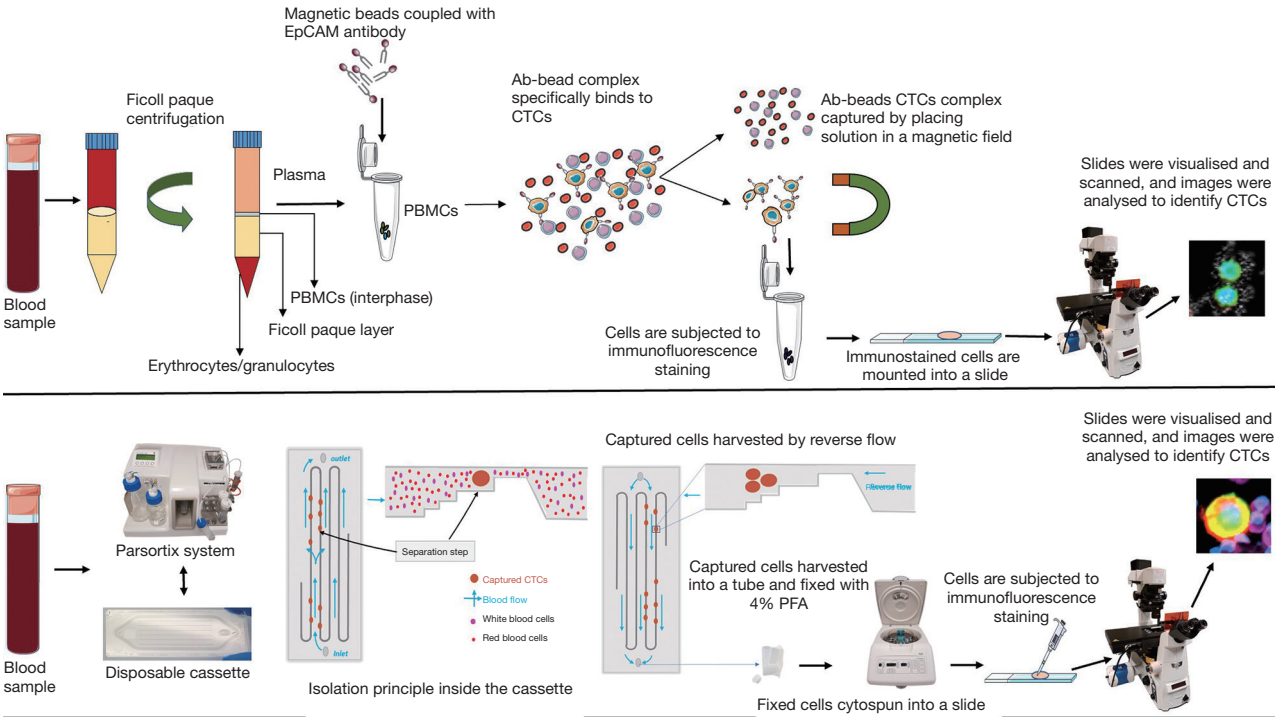

Figure 1 Workflow for assessment of PD-L1 expression on SCLC patient CTCs. CTC isolation workflow: blood is collected from SCLC patients and processed through Parsortix system and EpCAM-coated magnetic beads. Enriched cells are collected, permeabilised and fixed, and then immunostained with immunofluorescence markers for imaging. Medical elements in this image are from smart.servier.com. CTCs, circulating tumour cells; PBMCs, peripheral blood mononuclear cells; Ab-bead, antibody conjugated beads; PFA, paraformaldehyde; SCLC, small-cell lung cancer.

Methods

Patient recruitment and sample collection

For this pilot study, a total of 21 SCLC patients were recruited in the study between August 2018–March 2021 at Sir Charles Gairdner Hospital (SCGH) and Fiona Stanley Hospital (FSH) in Perth, Western Australia. Written informed consent was obtained from all patients under approved Human Research Ethics Committee protocols from Edith Cowan University (No. 18957) and Sir Charles Gairdner Hospital (No. 2013-246, RGS0000003289). The study was conducted in accordance with the Declaration of Helsinki (as revised in 2013). At least 8 mL of blood was collected from each patient into K2EDTA (BD, Franklin Lakes, NJ, USA) tubes for CTC analysis. Samples were processed within 6 hours of blood collection. Demographic and clinical information such as age, gender, disease stage, performance status, smoking status, number of metastases, and type of treatment of patients were collected. Smoking status was collected as smokers and non-smokers. The smokers included those who smoked at least 10 packs a year (i.e., one pack a day for 10 years) either former or current.

Enrichment and identification of CTCs

Plasma was isolated from samples by centrifugation for 20 minutes at 300 ×g before CTC enrichment with anti-EpCAM coated magnetic beads (Appendix 1). The CTC capture process was carried out using anti-EpCAM beads in a modified protocol developed in our laboratory (31). Captured cells were immunostained with antibody cocktail containing three mixed pan-cytokeratin antibodies to ensure broad cytokeratin coverage, CD45, CD16, and CD66b antibodies to exclude hematopoietic cells and anti-PD-L1 antibody (28.8) to detect PD-L1 expression as detailed in Appendix 1.

In parallel, another blood sample was processed using the Parsortix system at 99-mbar through a 6.5-µm cassette (*Figure 1*). Enriched cells were harvested according to the manufacturer's instructions and fixed for 10 minutes at room temperature with 4% paraformaldehyde (PFA). A total of

Table 1 Clinical and demographic characteristics of patients

Variables	Frequency (n)	Percentage (%)
Age (years), median (IQR)	67.5 (63.5–83.0)	–
Age group (years)		
<67	9	42.9
≥67	12	57.1
Gender		
Male	9	42.9
Female	12	57.1
Disease stage		
Limited	2	9.5
Extensive	19	90.5
Performance status (ECOG)		
0	9	42.9
1	8	38.1
≥2	4	19.0
Smoking status		
Yes	20	95.2
No	1	4.8
Number of metastasis		
1	5	23.8
≥2	16	76.2
Type of treatment		
Chemotherapy	7	33.3
Chemotherapy + ICI	13	61.9
Radiation	1	4.8

IQR, interquartile range; ECOG, Eastern Cooperative Oncology Group; ICI, immune checkpoint inhibitor.

8–9 mL of blood was processed through each method. To increase the numbers of markers to be interrogated, such as EpCAM expression separate from cytokeratins, vimentin, and PD-L1 expression (29), we adapted the quenching and re-staining protocol described by Adams *et al.* (32). This protocol utilises borohydride to quench fluorescent signals after an initial round of immunostaining followed by a second round of staining for additional markers, allowing for multi-phenotype analysis of CTCs. The PD-L1 detection, quenching, and restaining methods were standardised using MCF7, MCF7 induced with IFN-γ, MDA-MB-231 cell lines spiked into white blood cells (WBCs) from healthy control donors as detailed in Appendix 1.

Imaging and image analysis

Slides were visualised and scanned using a Nikon Eclipse Ti-E inverted fluorescent microscope (Nikon, Chiyoda, Japan). Images were analysed using the NIS-Elements Analysis software, version 5.21 (Nikon).

Statistical analysis

All data was entered into Microsoft Excel and analysed with GraphPad Prism (version 8.0.2). Demographic data is presented as numbers, ranges, or counts, percentages, means, and medians where applicable using GraphPad version 8. Cohen's kappa test was used to analyse the difference in CTC detection rates between EpCAM-coated magnetic beads and the Parsortix system as well as an agreement between the two isolation methods.

Survival analysis was performed using the Kaplan-Meier method and differences in patient survival rates were determined using log-rank tests. Univariate and multivariate Cox regression hazard models for OS were performed for CTC count, number of metastases, Eastern Cooperative Oncology Group (ECOG) performance status, sex, and age using SPSS version 26. All survival plots were performed in R (version 4.05) using the "survplot" package (33,34) with $P<0.05$ considered statistically significant.

Results

Clinical characteristics of patients

A total of 23 blood samples were collected from 21 SCLC patients for the analysis of the presence of CTCs before the commencement of treatment. Blood samples for CTC enumeration were collected before treatment in 19 patients, while bloods were collected before treatment and at the time of relapse in 2 patients. The clinical characteristics of the study population are summarised in *Table 1*. Of the 21 SCLC patients in this study, 2 patients (9.5%) had limited stage disease and 19 (90.5%) had extensive disease. The median age of SCLC patients at the time of diagnosis was 67.5 (range, 63.5–83.0) years and there were 12 females and 9 males. Patients were treated with chemotherapy alone (n=7) or in combination with either atezolizumab or durvalumab (n=13). One patient was treated with cyberknife radiation.

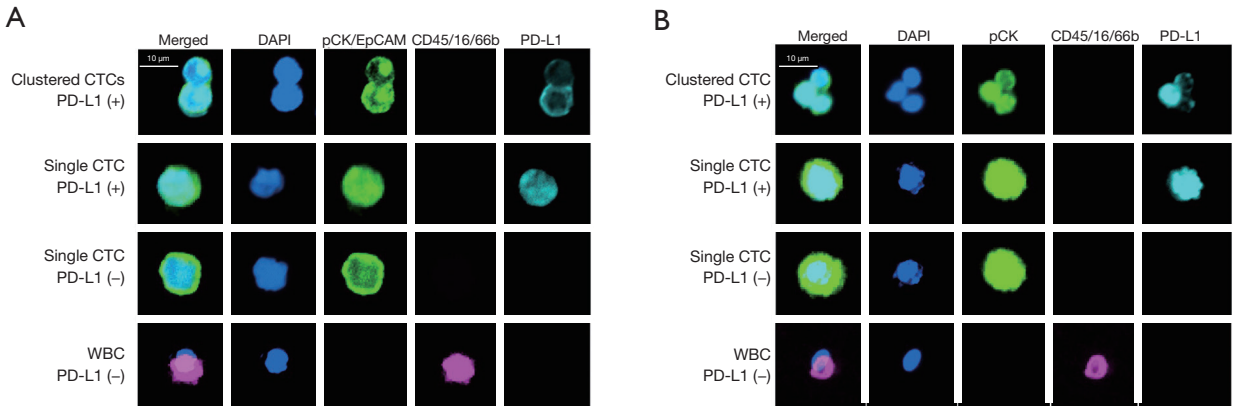

Figure 2 Representative images of SCLC CTCs identified by immunofluorescence staining. (A) CTCs enriched with Parsortix system. Cells were immunostained with pan-cytokeratins and EpCAM (green), CD45/16/66b (pink), and TSA PD-L1 (cyan). (B) CTCs enriched by EpCAM coated magnetic beads. Cells were immunostained with pan-cytokeratins (pCK, green), CD45/16/66b (pink), and TSA PD-L1 (cyan). WBC were included for comparison. Scale bar (top left) represents 10 µm. CTCs, circulating tumour cells; WBC, white blood cells; SCLC, small-cell lung cancer.

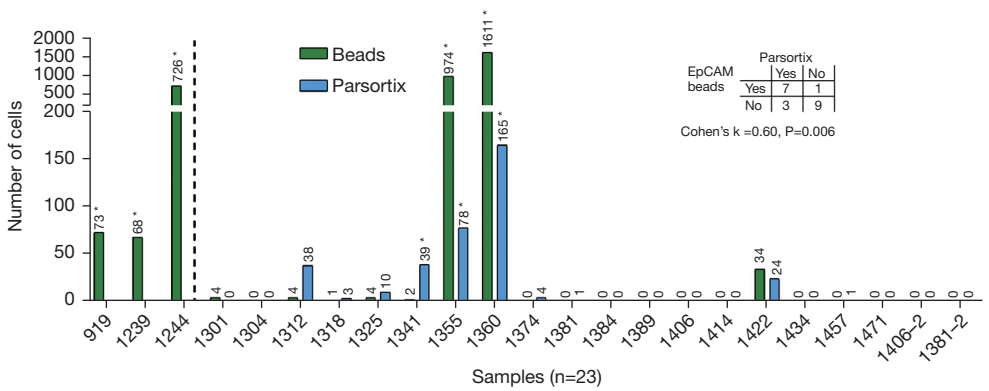

Figure 3 CTC counts in SCLC patients. Samples were processed with EpCAM-coated magnetic beads (n=23, green bars), and a proportion of them (to the right of the dashed line) was also enriched for CTCs using the Parsortix system (n=20, blue bars). The number of cells on each sample is indicated on top of the bars. *, indicate samples with CTC clusters. A contingency table comparing the number of positive samples by each method and associated statistics have been inserted. CTC, circulating tumour cell; SCLC, small-cell lung cancer.

CTC enumeration and characterisation

CTCs were isolated from 23 blood samples using anti-EpCAM immunomagnetic beads. Only 20 of these patients had a second blood sample available for CTC isolation using the Parsortix system. Enriched CTCs were identified through immunofluorescence staining, as exemplified in *Figure 2*. CTCs were detected in 11 of 23 (47.8%) samples processed with EpCAM-coated magnetic beads [median =5 (range, 1–1,611)] and in 10 of 20 (50.0%) samples processed with the Parsortix system [median =4 (range, 1–165) (*Figure 3*). Combining both methods, CTCs were found in 14/23 (60.9%) of the SCLC samples. Comparison of CTC detection in the 20 matched samples using Cohen's kappa coefficient indicated a moderate agreement (κ =0.51; P=0.017) between the detection rate of the two methods. In samples with a large number of CTCs (cases 1355 and 1360 in *Figure 3*), EpCAM beads recovered 10 times more CTC than using Parsortix. However, seven samples (1312, 1318, 1325, 1341, 1374, 1381 and 1457) exhibited a higher number of CTC recovered using the Parsortix system than

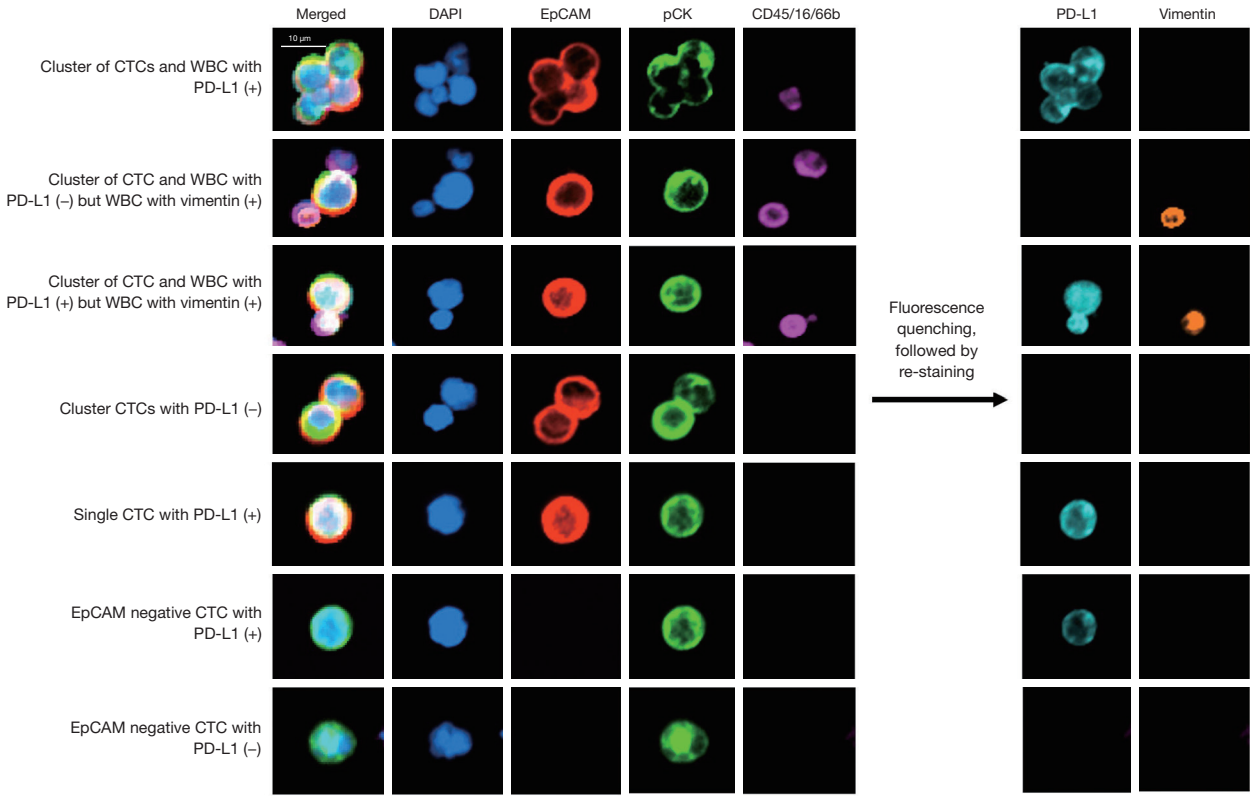

Figure 4 Representative cells enriched with the Parsortix system. Cells were stained with pan-cytokeratins (pCK, green), EpCAM (red), CD45/16/66b (pink) to identify classical SCLC CTCs, followed by fluorescence quenching and re-immunostained for PD-L1 expression (cyan) and vimentin (orange). Scale bar (top left) represents 10 µm. CTCs, circulating tumour cells; WBC, white blood cells; SCLC, small-cell lung cancer.

using EpCAM-coated beads.

CTC clusters were found in 6/23 of samples. Of the 6 samples with clusters, 3 samples were processed with EpCAM beads only. The remaining 3 cluster-containing samples were processed with both isolation methods, where clusters were found in all three Parsortix samples and 2/3 EpCAM beads samples (*Figure 3*). Additionally, we found WBCs paired with single CTCs or with CTC clusters in all 3 samples with clusters processed on the Parsortix system, but not in any of the EpCAM-captured samples (*Figure 4*, Figure S4). A subgroup of 14 samples enriched using Parsortix was also assessed for the expression of EpCAM and CK on CTCs separately, as well as for vimentin expression (*Figure 4*). No vimentin expressing CTCs were detected in any of the patients. A total of 17 EpCAM-negative CK-positive CTCs were detected in 3/14 (21.4%) patients, and these cells were always found as single CTCs (*Figure 4*, Figure S5). Notably, in one sample (1374 in *Figure 3*) only EpCAM-negative CTCs were detected, which was consistent with the sample found to be negative using the EpCAM-beads capturing approach.

PD-L1 expression on CTCs

PD-L1 expression was assessed on the 14 CTC-positive samples found among the 23 blood samples analysed. Overall, ≥2 PD-L1$^+$ CTCs were detected in 7/23 (30.4%) samples regardless of the isolation method. PD-L1$^+$ CTCs were found in 5 samples processed with EpCAM-coated magnetic beads and in 4 samples processed with Parsortix (*Figure 5*). PD-L1 expression was analysed on a total of 3,501 CTCs isolated with EpCAM-coated beads with 257 (7.3%) found positive for PD-L1. In comparison, 30 of 363 (8.3%) CTCs isolated on the Parsortix system expressed PD-L1. Three of the 17 EpCAM-negative CTCs identified were positive for PD-L1 expression.

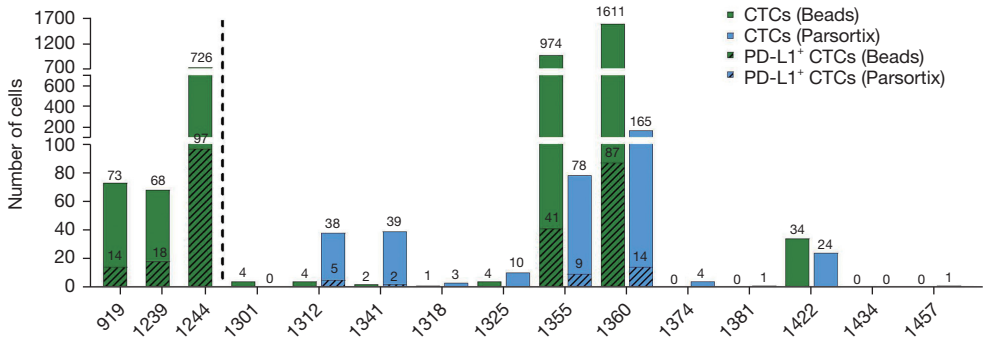

Figure 5 Comparison of PD-L1 expressing CTCs isolated by immunomagnetic beads and the Parsortix system. Bars represent counts in CTC positive samples processed with EpCAM-coated magnetic beads (n=15, green bars), and a proportion of them (to the right of the dashed line) was also enriched for CTCs using the Parsortix system (n=12, blue bars). PD-L1 positive CTC counts are indicated by hatched bars. CTCs, circulating tumour cells.

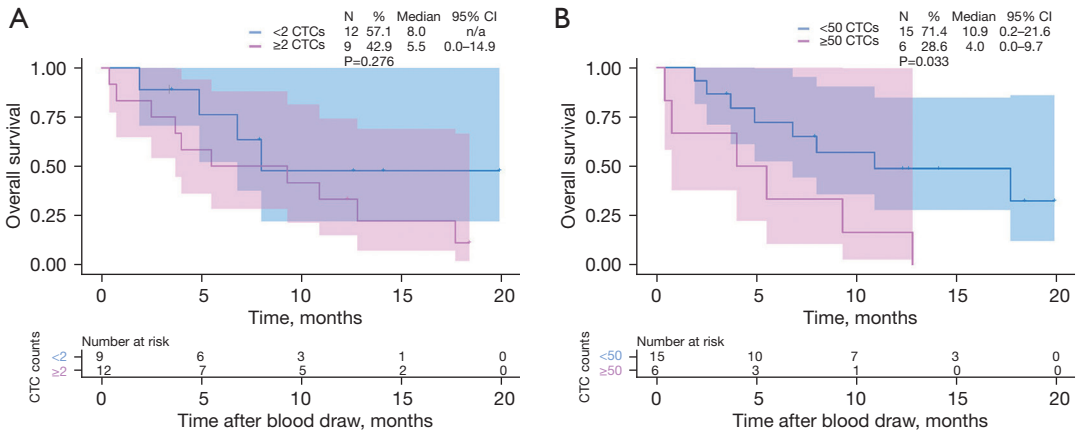

Figure 6 Kaplan-Meier curves for OS for analysed CTCs thresholds. (A) <2 *vs.* ≥2 CTCs. (B) <50 *vs.* ≥50 CTCs. Log-rank P values, group numbers, median, and 95% CIs are indicated for each plot. CTCs, circulating tumour cells; CI, confidence interval; OS, overall survival.

Survival analysis

The median OS of patients after blood draw was 9.3 months (95% CI: 4.3–14.2 months). We assessed the correlations of CTC counts with OS using the previously validated thresholds of 2 and 50 CTC per 7.5 mL of blood (24,35,36). Neither of the two CTC threshold groupings showed statistically significant differences between the clinical characteristic of the patients (Table S2). There was no statistically significant difference in median OS between patients with ≥2 CTCs compared to those with <2 CTCs (5.5 *vs.* 8 months, P=0.276). However, patients with ≥50 CTCs had significantly shorter median OS compared with those with <50 CTCs (4.0 *vs.* 10.9 months, P=0.033) (*Figure 6*). Univariate Cox regression analysis revealed that ≥50 CTCs was significantly associated with shorter OS (HR =3.11; 95% CI: 1.01–9.32; P=0.043). Multivariate analysis showed that ≥50 CTCs was an independent prognostic factor for shorter OS (HR =6.15; 95% CI: 1.35–27.99; P=0.019) (*Table 2*). Among the 14 SCLC patients with ≥2 CTCs, there was no statistical difference in the survival of patients with PD-L1-CTCs compared with patients with PD-L1+ CTCs (10.9 *vs.* 4.0 months, P=0.103) (Figure S6).

Discussion

CTCs have emerged as appealing liquid biopsy candidates that could enhance treatment decision-making (14,15). In this study, we employed a size-based CTC enrichment method, the Parsortix system, that has been demonstrated

Table 2 Univariate and multivariate Cox hazard regression analysis

Variables	Groups	Univariate		Multivariate	
		HR (95% CI)	P value	HR (95% CI)	P value
Age (years)	≥67 (n=12)	–	–	–	–
	<67 (n=9)	1.29 (0.43–3.87)	0.641	1.14 (0.27–4.77)	0.858
Sex	Male (n=9)	–	–	–	–
	Female (n=12)	2.14 (0.17–6.50)	0.176	2.45 (0.64–9.35)	0.189
CTC count	<50 (n=15)	–	–	–	–
	≥50 (n =6)	3.11 (1.01–9.32)	0.043*	6.15 (1.35–27.99)	0.019*
Performance status (ECOG)	0 (n=9)	–	–	–	–
	1 (n=8)	1.26 (0.38–4.18)	0.194	0.45 (0.09–2.25)	0.337
	≥2 (n=4)	2.62 (0.61–11.23)	0.480	4.23 (0.64–27.98)	0.134
No of metastases	1 (n=5)	–	–	–	–
	≥2 (n=16)	2.79 (0.59–13.02)	0.230	3.56 (0.62–20.48)	0.156

*, P<0.05, considered statistically significant. HR, hazard ratio; CI, confidence interval; ECOG, Eastern Cooperative Oncology Group.

to harvest CTCs in a greater proportion in different tumour types including SCLC (29,37-39). We also validated a simple, rapid, and affordable method to detect CTCs based on magnetic cell separation. We compared CTCs detection rates between the two isolation methods, using matched samples, and evaluated the potential of CTCs for PD-L1 expression other than SCLC biopsy tissue.

Both epitope-dependent and epitope-independent enrichment methods have been shown to isolate high numbers of CTCs in SCLC patients compared with other types of cancers (40). The overall frequency of patients with detectable CTCs in our study was 61%, in line with previous reports in SCLC, showing detectable CTCs in between 60–95% of patients. However, CTC detection rate was higher in samples processed with the Parsortix system (55%) compared to EpCAM-coated magnetic beads (48%) in a matched comparison. Chudziak *et al.* (29) also reported similar results reporting that cytokeratin positive CTCs were detectable in all the 12 samples processed on the Parsortix platform while CellSearch only detected cytokeratin positive CTCs in 10 (83%) of the SCLC patients tested. These results may be explained by the fact that EpCAM-based isolation methods may fail to capture EpCAM low/negative expressing CTCs. In line with this, we demonstrated here that EpCAM negative CTCs were isolated using Parsortix in 14.3% of the processed samples. On the other hand, the number of Parsortix-isolated CTCs was lower those isolated using EpCAM-beads, in particular for the two patients with the largest number of CTCs. SCLC CTCs are relatively small, compared to other carcinomas (ref) and may not be efficiently retained by the Parsortix system which isolates CTCs based on size and deformability (41).

It has been proposed that primary and metastatic tumours release cells into the bloodstream through a process of the epithelial to mesenchymal transition (EMT) (42). Given the loss of EpCAM observed in CTCs isolated using Parsortix, we assessed the potential expression of vimentin on these cells. Results revealed the absence of vimentin in all the CTCs interrogated. This result suggests that EMT is not homogenously expressed in tumour cells within the circulation of SCLC patients and supports the importance of other types of motility shift such as amoeboid cell invasion which has been demonstrated to be typical of SCLC (43,44). Although, there are limited studies on amoeboid tumour cell invasion in SCLC and lack of EMT markers such as vimentin on SCLC CTCs suggest it might be an important subject area for further studies.

Multiple studies in the last decade have demonstrated that the presence of measurable CTCs in SCLC patients is associated with shorter survival (24,36,45). The presence of ≥2 and ≥50 CTCs per 7.5 mL of blood from SCLC patients before chemotherapy was highly significant for poor OS, regardless of other clinical prognostic variables (24,36).

Consistent with these studies (24,36,45), we found that patients with ≥50 CTCs had significantly shorter median OS compared with the <50 CTCs group.

The biology of clustered CTCs is an evolving area of research. CTC clusters in the peripheral blood have been reported in patients with SCLC (24). In this study, CTC clusters were detected samples processed on the Parsortix system and with EpCAM coated magnetic beads. The number of cells within the CTC clusters detected on the Parsortix were large, comprised of up to 8 CTCs and involving WBCs, compared to 2–3 clustered CTCs detected using the immunomagnetic beads. A number of studies have shown the role of clusters in the migration and survival of CTCs in breast and gastric cancer (38,46,47). However, no studies have directly addressed how SCLC CTC clusters may enable metastases and/or chemoresistance.

Until recently, far too little attention has been paid to the expression of PD-L1 on CTCs in SCLC, compared to its extensive study in NSCLC (30,48-51). This is partly due to the early approval of ICIs for the treatment of NSCLC and higher expression of PD-L1 protein in NSCLC. On the other hand, there is a wide difference in the prevalence of PD-L1 expression in tumour cells of SCLC patients reported in the literature, ranging from 0–86% (52,53). Even though ICIs combined with chemotherapy were recently approved for SCLC treatment, tumour PD-L1 expression has been demonstrated to be a non-discriminatory biomarker (8,9,11). However, it is possible that retaining PD-L1 might represent one of the mechanisms that CTCs use to survive immune system attack while in circulation and, therefore a better readout of a pre-existing anti-tumour response. Previous studies in melanoma and NSCLC have shown that PD-L1 expression on CTCs a promising prognostic biomarker in patients treated with ICIs, despite the lack of correlation with the expression on matching tumours (54,55).

Our study is the first to evaluate PD-L1 expression on CTCs in SCLC by both epitope-dependent and -independent enrichment techniques. Two other studies have assessed the expression of PD-L1 on CTCs in SCLC patients finding PD-L1 expression in 0–50% of samples (49,51). In our study, ≥2 PD-L1$^+$ CTCs were detected in 7/23 (30.4%) samples regardless of the isolation method. This discrepancy could be attributed to the antibody clones utilised, especially the high sensitivity of the PD-L1 antibody clone (28.8) or TSA amplification of the antibody signal for PD-L1 detection in our study.

The present study has some limitations such as the fact that the study population was small with an inferred post-hoc power of 0.36, which hindered the feasibility of inferential statistics. In particular, the inclusion of a small number of patients treated with chemotherapy alone did not enable an analysis of the predictive value of PD-L1 expressing CTC for response to treatment as shown for other cancers (37,56,57). It was not possible to assess the association of PD-L1$^+$ CTCs with survival among patients treated with immunotherapy, given their small number of cases (9 of 21) in this subgroup. Finally, PD-L1 expression assessment is not a routine practice for SCLC. Thus, we could not compare the expression of PD-L1 on CTCs to that of the matching tumours as samples were not available for evaluation.

Conclusions

The current findings extend our knowledge of the ability of epitope-independent technologies to detect subsets of CTCs. The study demonstrates that PD-L1 expression can be quantified on CTCs detected in SCLC patients. This could potentially serve as a marker to evaluate the likelihood of anti-PD-1 therapy response.

Acknowledgments

We thank healthy volunteers and patients for the provision of samples for this study. We also acknowledge the phlebotomy and nursing staff of participating hospitals in acquiring blood samples, and all the team members that helped with sample collection and transportation. We would like to also acknowledge Servier Medical Art (https://smart.servier.com) for the provision of medical elements for Figure 1.

Funding: EA is supported by Edith Cowan University PhD Scholarship. ESG is supported by a fellowship from the Cancer Council of Western Australia. ABB is supported by an Edith Cowan University Postgraduate Scholarship and a Cancer Council of Western Australia PhD Top-up Scholarship. The study was partially supported by the Cancer Research Trust 'Enabling advanced single-cell cancer genomics in WA' grant.

Footnote

Reporting Checklist: The authors have completed the MDAR reporting checklist. Available at https://tlcr.amegroups.com/article/view/10.21037/tlcr-21-819/rc

Data Sharing Statement: Available at https://tlcr.amegroups.com/article/view/10.21037/tlcr-21-819/dss

Peer Review File: Available at https://tlcr.amegroups.com/article/view/10.21037/tlcr-21-819/prf

Conflicts of Interest: All authors have completed the ICMJE uniform disclosure form (available at https://tlcr.amegroups.com/article/view/10.21037/tlcr-21-819/coif). SB reports to be an Advisory Board Member for Sanofi and Eli Lilly and has received conference attendance support by Merck Sharp & Dohme; MMi reports to be an Advisory Board Member (lung cancer, immune-oncology) for Pfizer, Roche, AstraZeneca, Takeda, Merck Sharp & Dohme, Bristol-Myers Squibb, Novartis, The Limbic, Guardant Health, and BeiGene; has received travel support from AstraZeneca, and has been part of the Data Safety Monitoring Board of a Novartis clinical trial; ESG is supported by a fellowship from the Cancer Council of Western Australia and a Cancer Research Trust; has received specialized technical support provided by Angle Parsortix. The other authors have no conflicts of interest to declare.

Ethical Statement: The authors are accountable for all aspects of the work in ensuring that questions related to the accuracy or integrity of any part of the work are appropriately investigated and resolved. Written informed consent was obtained from all patients under approved Human Research Ethics Committee protocols from Edith Cowan University (No. 18957) and Sir Charles Gairdner Hospital (No. 2013-246, RGS0000003289). The study was conducted in accordance with the Declaration of Helsinki (as revised in 2013).

References

1. Bray F, Ferlay J, Soerjomataram I, et al. Global cancer statistics 2018: GLOBOCAN estimates of incidence and mortality worldwide for 36 cancers in 185 countries. CA Cancer J Clin 2018;68:394-424.
2. Nicholson AG, Chansky K, Crowley J, et al. The International Association for the Study of Lung Cancer Lung Cancer Staging Project: Proposals for the Revision of the Clinical and Pathologic Staging of Small Cell Lung Cancer in the Forthcoming Eighth Edition of the TNM Classification for Lung Cancer. J Thorac Oncol 2016;11:300-11.
3. Shepherd FA, Crowley J, Van Houtte P, et al. The International Association for the Study of Lung Cancer lung cancer staging project: proposals regarding the clinical staging of small cell lung cancer in the forthcoming (seventh) edition of the tumor, node, metastasis classification for lung cancer. J Thorac Oncol 2007;2:1067-77.
4. Sundstrøm S, Bremnes RM, Kaasa S, et al. Cisplatin and etoposide regimen is superior to cyclophosphamide, epirubicin, and vincristine regimen in small-cell lung cancer: results from a randomized phase III trial with 5 years' follow-up. J Clin Oncol 2002;20:4665-72.
5. American Cancer Society. Cancer treatment and survivorship facts & figures 2014–2015. Atlanta, GA, USA: American Cancer Society, 2014.
6. Waqar SN, Morgensztern D. Treatment advances in small cell lung cancer (SCLC). Pharmacol Ther 2017;180:16-23.
7. Takada M, Fukuoka M, Kawahara M, et al. Phase III study of concurrent versus sequential thoracic radiotherapy in combination with cisplatin and etoposide for limited-stage small-cell lung cancer: results of the Japan Clinical Oncology Group Study 9104. J Clin Oncol 2002;20:3054-60.
8. Antonia SJ, López-Martin JA, Bendell J, et al. Nivolumab alone and nivolumab plus ipilimumab in recurrent small-cell lung cancer (CheckMate 032): a multicentre, open-label, phase 1/2 trial. Lancet Oncol 2016;17:883-95.
9. Horn L, Mansfield AS, Szczęsna A, et al. First-Line Atezolizumab plus Chemotherapy in Extensive-Stage Small-Cell Lung Cancer. N Engl J Med 2018;379:2220-9.
10. Pedoeem A, Azoulay-Alfaguter I, Strazza M, et al. Programmed death-1 pathway in cancer and autoimmunity. Clin Immunol 2014;153:145-52.
11. Paz-Ares L, Dvorkin M, Chen Y, et al. Durvalumab plus platinum-etoposide versus platinum-etoposide in first-line treatment of extensive-stage small-cell lung cancer (CASPIAN): a randomised, controlled, open-label, phase 3 trial. Lancet 2019;394:1929-39.
12. McLaughlin J, Han G, Schalper KA, et al. Quantitative

Assessment of the Heterogeneity of PD-L1 Expression in Non-Small-Cell Lung Cancer. JAMA Oncol 2016;2:46-54.
13. McLean AEB, Barnes DJ, Troy LK. Diagnosing Lung Cancer: The Complexities of Obtaining a Tissue Diagnosis in the Era of Minimally Invasive and Personalised Medicine. J Clin Med 2018;7:163.
14. Nurwidya F, Zaini J, Putra AC, et al. Circulating Tumor Cell and Cell-free Circulating Tumor DNA in Lung Cancer. Chonnam Med J 2016;52:151-8.
15. Alix-Panabières C, Pantel K. Clinical Applications of Circulating Tumor Cells and Circulating Tumor DNA as Liquid Biopsy. Cancer Discov 2016;6:479-91.
16. Keller L, Pantel K. Unravelling tumour heterogeneity by single-cell profiling of circulating tumour cells. Nat Rev Cancer 2019;19:553-67.
17. Pantel K, Alix-Panabières C. Circulating tumour cells in cancer patients: challenges and perspectives. Trends Mol Med 2010;16:398-406.
18. Friedl P, Locker J, Sahai E, et al. Classifying collective cancer cell invasion. Nat Cell Biol 2012;14:777-83.
19. Liu X, Taftaf R, Kawaguchi M, et al. Homophilic CD44 Interactions Mediate Tumor Cell Aggregation and Polyclonal Metastasis in Patient-Derived Breast Cancer Models. Cancer Discov 2019;9:96-113.
20. Hamilton G, Burghuber O, Zeillinger R. Circulating tumor cells in small cell lung cancer: ex vivo expansion. Lung 2015;193:451-2.
21. Hodgkinson CL, Morrow CJ, Li Y, et al. Tumorigenicity and genetic profiling of circulating tumor cells in small-cell lung cancer. Nat Med 2014;20:897-903.
22. Hamilton G, Moser D, Hochmair M. Metastasis: Circulating Tumor Cells in Small Cell Lung Cancer. Trends Cancer 2016;2:159-60.
23. Zhang J, Wang HT, Li BG. Prognostic significance of circulating tumor cells in small--cell lung cancer patients: a meta-analysis. Asian Pac J Cancer Prev 2014;15:8429-33.
24. Hou JM, Krebs MG, Lancashire L, et al. Clinical significance and molecular characteristics of circulating tumor cells and circulating tumor microemboli in patients with small-cell lung cancer. J Clin Oncol 2012;30:525-32.
25. Chudasama DY, Freydina DV, Freidin MB, et al. Inertia based microfluidic capture and characterisation of circulating tumour cells for the diagnosis of lung cancer. Ann Transl Med 2016;4:480.
26. Ferreira MM, Ramani VC, Jeffrey SS. Circulating tumor cell technologies. Mol Oncol 2016;10:374-94.
27. Bailey PC, Martin SS. Insights on CTC Biology and Clinical Impact Emerging from Advances in Capture Technology. Cells 2019;8:553.
28. Rawal S, Yang YP, Cote R, et al. Identification and Quantitation of Circulating Tumor Cells. Annu Rev Anal Chem (Palo Alto Calif) 2017;10:321-43.
29. Chudziak J, Burt DJ, Mohan S, et al. Clinical evaluation of a novel microfluidic device for epitope-independent enrichment of circulating tumour cells in patients with small cell lung cancer. Analyst 2016;141:669-78.
30. Acheampong E, Spencer I, Lin W, et al. Is the Blood an Alternative for Programmed Cell Death Ligand 1 Assessment in Non-Small Cell Lung Cancer? Cancers (Basel) 2019;11:920.
31. Freeman JB, Gray ES, Millward M, et al. Evaluation of a multi-marker immunomagnetic enrichment assay for the quantification of circulating melanoma cells. J Transl Med 2012;10:192.
32. Adams DL, Alpaugh RK, Tsai S, et al. Multi-Phenotypic subtyping of circulating tumor cells using sequential fluorescent quenching and restaining. Sci Rep 2016;6:33488.
33. R: a language and environment for statistical computing. Team RC, 2013.
34. IBM SPSS Statistics for Windows, Version 22.0. Armonk, NY, USA: IBM Corp., 2013.
35. Tay RY, Fernández-Gutiérrez F, Foy V, et al. Prognostic value of circulating tumour cells in limited-stage small-cell lung cancer: analysis of the concurrent once-daily versus twice-daily radiotherapy (CONVERT) randomised controlled trial. Ann Oncol 2019;30:1114-20.
36. Igawa S, Gohda K, Fukui T, et al. Circulating tumor cells as a prognostic factor in patients with small cell lung cancer. Oncol Lett 2014;7:1469-73.
37. Janning M, Kobus F, Babayan A, et al. Determination of PD-L1 Expression in Circulating Tumor Cells of NSCLC Patients and Correlation with Response to PD-1/PD-L1 Inhibitors. Cancers (Basel) 2019;11:835.
38. Szczerba BM, Castro-Giner F, Vetter M, et al. Neutrophils escort circulating tumour cells to enable cell cycle progression. Nature 2019;566:553-7.
39. Aya-Bonilla CA, Morici M, Hong X, et al. Detection and prognostic role of heterogeneous populations of melanoma circulating tumour cells. Br J Cancer 2020;122:1059-67.
40. De Luca A, Gallo M, Esposito C, et al. Promising Role of Circulating Tumor Cells in the Management of SCLC. Cancers (Basel) 2021;13:2029.
41. Miller MC, Robinson PS, Wagner C, et al. The Parsortix™ Cell Separation System-A versatile liquid biopsy platform. Cytometry A 2018;93:1234-9.

42. Ito T, Kudoh S, Ichimura T, et al. Small cell lung cancer, an epithelial to mesenchymal transition (EMT)-like cancer: significance of inactive Notch signaling and expression of achaete-scute complex homologue 1. Hum Cell 2017;30:1-10.
43. Rintoul RC, Sethi T. Extracellular matrix regulation of drug resistance in small-cell lung cancer. Clin Sci (Lond) 2002;102:417-24.
44. van Zijl F, Krupitza G, Mikulits W. Initial steps of metastasis: cell invasion and endothelial transmigration. Mutat Res 2011;728:23-34.
45. Naito T, Tanaka F, Ono A, et al. Prognostic impact of circulating tumor cells in patients with small cell lung cancer. J Thorac Oncol 2012;7:512-9.
46. Aceto N, Bardia A, Miyamoto DT, et al. Circulating tumor cell clusters are oligoclonal precursors of breast cancer metastasis. Cell 2014;158:1110-22.
47. Chen Y, Yuan J, Li Y, et al. Profiling heterogenous sizes of circulating tumor microemboli to track therapeutic resistance and prognosis in advanced gastric cancer. Hum Cell 2021;34:1446-54.
48. Guibert N, Delaunay M, Lusque A, et al. PD-L1 expression in circulating tumor cells of advanced non-small cell lung cancer patients treated with nivolumab. Lung Cancer 2018;120:108-12.
49. Ilie M, Hofman V, Long E, et al. PD-L1 expression in primary tumor and circulating tumor cells in patients with small cell lung carcinomas. Cancer Res 2016;76:Abstract nr 2220.
50. Nicolazzo C, Raimondi C, Mancini M, et al. Monitoring PD-L1 positive circulating tumor cells in non-small cell lung cancer patients treated with the PD-1 inhibitor Nivolumab. Sci Rep 2016;6:31726.
51. Boffa DJ, Graf RP, Salazar MC, et al. Cellular Expression of PD-L1 in the Peripheral Blood of Lung Cancer Patients is Associated with Worse Survival. Cancer Epidemiol Biomarkers Prev 2017;26:1139-45.
52. Acheampong E, Abed A, Morici M, et al. Tumour PD-L1 Expression in Small-Cell Lung Cancer: A Systematic Review and Meta-Analysis. Cells 2020;9:2393.
53. Sun Y, Zhai C, Chen X, et al. Characterization of PD-L1 protein expression and CD8+ tumor-infiltrating lymphocyte density, and their associations with clinical outcome in small-cell lung cancer. Transl Lung Cancer Res 2019;8:748-59.
54. Dall'Olio FG, Gelsomino F, Conci N, et al. PD-L1 Expression in Circulating Tumor Cells as a Promising Prognostic Biomarker in Advanced Non-small-cell Lung Cancer Treated with Immune Checkpoint Inhibitors. Clin Lung Cancer 2021;22:423-31.
55. Kulasinghe A, Kapeleris J, Cooper C, et al. Phenotypic Characterization of Circulating Lung Cancer Cells for Clinically Actionable Targets. Cancers (Basel) 2019;11:380.
56. Khattak MA, Reid A, Freeman J, et al. PD-L1 Expression on Circulating Tumor Cells May Be Predictive of Response to Pembrolizumab in Advanced Melanoma: Results from a Pilot Study. Oncologist 2020;25:e520-7.
57. Sinoquet L, Jacot W, Gauthier L, et al. Programmed Cell Death Ligand 1-Expressing Circulating Tumor Cells: A New Prognostic Biomarker in Non-Small Cell Lung Cancer. Clin Chem 2021;67:1503-12.

Cite this article as: Acheampong E, Abed A, Morici M, Spencer I, Beasley AB, Bowyer S, Asante DB, Lomma C, Lin W, Millward M, Gray ES. Evaluation of PD-L1 expression on circulating tumour cells in small-cell lung cancer. Transl Lung Cancer Res 2022;11(3):440-451. doi: 10.21037/tlcr-21-819

Appendix 1

Cell lines

Carcinoma-derived cell lines MCF7 and MDA-MB-231 (breast cancer), and LNCaP acquired from ATCC (ATCC, Manassas, VA, USA) were maintained in cell culture media as a monolayer at 37 ℃ with 5% CO_2 in humidified air. LNCaP cells were cultured in RPMI 1640 (ThermoFisher Scientific, Waltham, MA, USA), containing 10% foetal bovine serum (FBS) (ThermoFisher Scientific). MDA-MB-231 and MCF-7 cell lines were cultured in DMEM (ThermoFisher Scientific) containing 10% FBS. Cells were harvested at 80% confluency for flow cytometry and immunofluorescent staining. Some MCF7 cells were incubated with 100 ng/mL IFN-γ for 24 hours to induce PD-L1 expression.

Antibody purification, immunomagnetic beads coupling, and recovery assessment

Anti-EpCAM antibody (Ber-EP4, ab7504, Abcam) was purified using the NAb Spin Kits, 0.2 mL (ThermoFisher Scientific) following the manufacturer's instructions. Purified Anti-EpCAM antibody was covalently bound to magnetic beads using a Dynabead Antibody Coupling Kit (ThermoFisher Scientific) following the manufacturer's instructions. Purified antibody was quantified using a NanoDrop One (ThermoFisher Scientific); 3 µg of antibody was used per mg of Dynabeads M-270 Epoxy. Antibody coupling with the Dynabeads was confirmed using flow cytometry. For this, two microlitres of coated beads were added to 500 µL of phosphate-buffered saline (PBS) and incubated for 15 minutes at room temperature with a donkey anti-mouse IgG antibody conjugated to Alexa Fluor 488 (Abcam USA) diluted 1/500. After washing, beads were analysed using a Gallios Flow Cytometer (Beckman Coulter, Brea, CA, USA). Unlabelled EpCAM-coated beads were used as a negative control.

We assessed the performance of the EpCAM-coated magnetic beads and obtained 82% recovery efficiency using LNCaP cell lines (expressed EpCAM and CK), pre-labelled with 1 µL of CellTracker Red (ThermoFisher Scientific) spiked into peripheral blood mononuclear cells (PBMCs) obtained from healthy donors.

Assessment of PD-L1 expression by flow cytometry

PD-L1 expression for each cell line was initially assessed by flow cytometry using a Gallios Flow Cytometer (Beckman Coulter) with the 28.8 PD-L1 antibody clone (Abcam, Cambridge, UK). Ten thousand cells were suspended in 100 µL of stain buffer [1% bovine serum albumin (BSA)/10% normal donkey serum (NDS) in PBS] containing PD-L1 diluted 1/100 for 30 minutes. The cells were then washed once with 0.5% BSA in PBS before resuspending in stain buffer containing a secondary donkey anti-rabbit IgG antibody conjugated to Alexa Fluor® 488 (Abcam) diluted 1/500 for 30 minutes. The cells were once again washed once in 0.5% BSA in PBS before being resuspended in 100 µL of stain buffer and analysed using a Gallios Flow Cytometer (Beckman Coulter). Fluorescence values obtained for each cell line were then compared to form a relative scale which was utilised to identify high, low, and negative PD-L1 expressing cell lines which were subsequently used as controls Figure S1.

MDA-MB-231 cells constitutively expressed high levels of PD-L1, with a 9.2-fold shift in median fluorescence intensity relative to the isotype control. LnCAP cells had no apparent shift in median fluorescence intensity. MCF7 cells incubated with 100 ng/mL of IFN-γ for 24 hours had a 3.7-fold shift in median fluorescence intensity relative to the primary control. Therefore, MDA-MB-231 cell line was selected as the high expression control, IFN-γ induced MCF7 was selected as the low expression control and LnCAP was selected as the negative control.

Assessment of PD-L1 expression on cells captured using anti-EpCAM coated magnetic beads

Peripheral blood mononuclear cells (PBMCs) were isolated from blood by density gradient centrifugation over Ficoll-Paque (GE Healthcare Biosciences, Uppsala, Sweden) and resuspended in 1 mL MACS buffer (0.5% BSA, 2 mM EDTA in PBS, pH 7.2). Healthy control PBMC spiked MCF-7, induced with IFNγ to express PD-L1, was then isolated using 3 µL EpCAM antibody conjugated magnetic beads. Captured cells were quenched for endogenous peroxidase activity with 0.3% H_2O_2 for

https://dx.doi.org/10.21037/tlcr-21-819

20 minutes before incubated for 1 hour at room temperature with anti-pan cytokeratins, WBC marker, and unconjugated anti-PD-L1 antibody (Table S1) and then placed on a magnetic for 2 minutes. The resulting pellet was washed twice with PBS then incubated in stain buffer containing anti-rabbit horseradish peroxidase (HRP) (1/200, Perkin Elmer) for 30 minutes. Cells were again washed with PBS before incubating in TSA Plus working solution (TSA plus Cy5 kit, Perkin Elmer) for 5 minutes. The cells were once again washed with PBS and then placed on a magnetic. The resulting pellet was mounted with Fluoromount Gold plus DAPI (ThermoFisher Scientific). Tyramide signal amplification (TSA) was introduced to increase the signal for PD-L1 detection. Slides were visualised and scanned using a Nikon Eclipse Ti-E inverted fluorescent microscope. Images were analysed using the NIS-Elements Analysis software, version 5.21. Examples in Figure S2.

Carcinoma immunocytochemistry assay for PD-L1 expression on cytospun cells

MDA-MB-231 (strong PD-L1 expression), IFN-γ induced MCF-7 (weak PD-L1 expression), MCF7 (negative PD-L1 expression) cell line spikes were analyzed for PD-L1 expression. After collection, cell line spikes were immediately fixed in 4% paraformaldehyde (PFA) for 10 minutes. After that, cells were cytospun using Cytospin™ 4 (Thermo Fisher Scientific) onto glass slides at 2,000 rpm for 5 minutes at medium acceleration. Cells were then dried, and slides stored in a desiccator at 4 ℃ or progressed straight to staining. Cells were incubated in blocking buffer (10% NDS/10% Glycine/5% Human FcR block/3% BSA/0.2% TX in PBS) for 15 minutes before incubating in stain buffer (10% NDS/3% BSA/0.2% TX in PBS) containing pan-cytokeratins, WBCs markers (Table S1) for 1 hour. Following this incubation cells were washed in 1% BSA in PBS followed by washes in PBS. They were then incubated with 2 µL/mL of the nuclei staining dye solution, Hoechst 33342 (Thermo Fisher Scientific), for 15 minutes and finally wash with PBS.

A silicon isolator was immediately placed on the glass slide encircling the area where the cells were located. PBS (200 µL) was added to the space containing the cells, and the cells were immediately visualized and scanned using an inverted fluorescent microscope (Eclipse Ti-E, Nikon®, Japan). Images were analysed using the NIS-Elements High Content Analysis software, version 4.2.

After microscopy, the silicon isolator was removed, slides were washed five times for 5 minutes each in PBS before incubation in freshly prepared 1 mg/mL NaBH4 in PBS solution for 180 minutes, with the NaBH4 in PBS solution being replaced with fresh solution after 90 minutes. Slides were then washed five times for 5 minutes each in PBS before incubating in 100 mM tris solution for 1 hour. Slides were once again washed three times for 5 minutes each in PBS before quenching endogenous peroxidase activity with 0.3% H2O2 for 20 minutes. Slides were incubated in blocking buffer for 15 minutes before incubating in stain buffer containing PD-L1 (clone 28.8, Abcam) and Alexa Fluor 647 labelled anti-vimentin for 1 hour.

Slides were then washed three times with 1% BSA in PBS for 5 minutes each and then incubated in stain buffer containing anti-rabbit HRP (1/200, Perkin Elmer) for 30 minutes. Slides were again washed three times with 1% BSA in PBS for 5 minutes each before incubating in TSA Plus working solution (TSA plus Cy5 kit, Perkin Elmer) for 5 minutes. Finally, slides were once again washed three times with 1% BSA in PBS for 5 minutes each, washed once in PBS for 5 minutes, dried and mounted with Fluoromount Gold plus DAPI (ThermoFisher Scientific) for re-imagining.

MCF7 cells demonstrated strong CK/EpCAM staining and no detectable vimentin staining while MDA-MB-231 cells demonstrated weak CK/EpCAM staining and strong vimentin staining. PD-L1 was expressed at low levels in the IFN-γ induced MCF7 cells and strongly expressed in the MDA-MB-231 cells. All MCF7 cells, both IFN-γ induced and not, and all MDA-MB-231 cells were negative for the WBC markers CD16, CD66b, and CD45. This protocol was applied for the analysis of CTCs enriched using the Parsortix system (Figure S3).

https://dx.doi.org/10.21037/tlcr-21-819

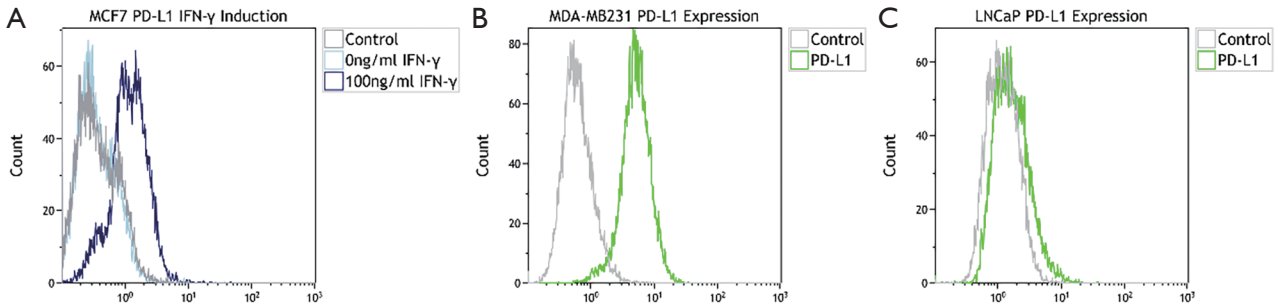

Figure S1 Histogram plots from flow cytometric analysis of PD-L1 expression on MCF7 cells (A), MDA-MB-231 cells (B) and LNCaP cells (C) using the 28.8 antibody diluted 1/100 with AF488 conjugated donkey anti-rabbit secondary antibody diluted 1/500. Cells stained with donkey anti-rabbit secondary antibody, but no primary antibody, were used as controls. MCF7 cells were analysed with and without induction of PD-L1 expression by incubation with IFN-γ for 24 hours.

Table S1 Antibodies used for immunocytochemistry staining

Antibody	Host species	Conjugate	Clone	Antigen location	Supplier (CTLG no.)	Dilution	Use
CD16	Mouse	AF647	3G8	Membrane	BioLegend USA, (302008)	1/50	WBC identification
CD45	Mouse	AF647	HI30	Membrane	BioLegend USA (304018)	1/50	WBC identification
CD66b	Mouse	AF647	G10F5	Membrane	BioLegend USA (305110)	1/100	WBC identification
Cytokeratins	Mouse	FITC	CK3-6H5	Cytoskeleton	Miltenyi Biotech Gladbach, Germany (130-118-964)	1/50	CTC identification
Cytokeratins	Mouse	AF488	C11	Cytoskeleton	Cell Signalling Technology, USA (4523S)	1/100	CTC identification
Cytokeratins	Mouse	AF488	AE1/AE3	Cytoskeleton	ThermoFisher Scientific, USA, (53-9003-80)	1/200	CTC identification
EpCAM	Mouse	PE	VU-1D9	Membrane	ThermoFisher Scientific, USA, (MA1-10197)	1/100	CTC identification
Vimentin	Mouse	AF647	V9	Cytoskeleton	Abcam, USA, (ab195878)	1/1,000	CTC identification
PD-L1	Rabbit	n/a	28.8	Membrane	Abcam, USA, (ab205921)	1/400	PD-L1 expression
HRP	Rabbit	n/a		n/a	Perkin Elmer	1/200	Signal amplification
TSA					TSA plus Cy5 kit, Perkin Elmer	1/50	Signal amplification

AF, Alexa Fluor; WBC, white blood cells; CTC, circulating tumour cell; PE, phycoerythrin; HRP, horseradish peroxidase.

https://dx.doi.org/10.21037/tlcr-21-819

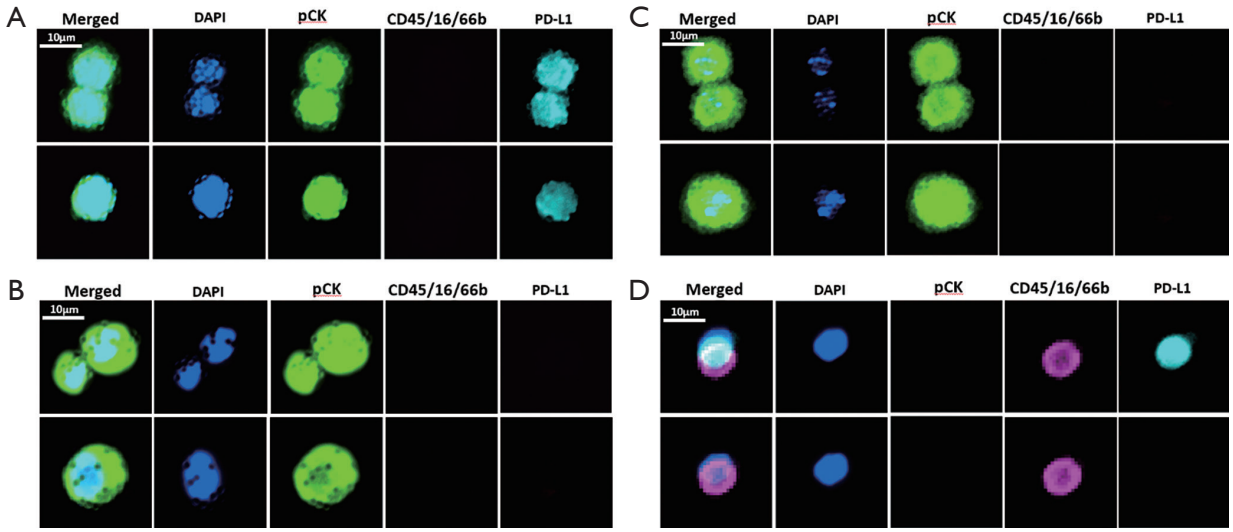

Figure S2 Immunofluorescence staining of beads recovered cells. Representative images of IFN-γ induced MCF7 cells (A), non-induced MCF7 cells (B), LnCaP cells (C) and WBCs (D). Cells were stained with antibodies targeting mixed pan-cytokeratins (pCK, green), AF647 CD45/CD16/CD66b (pink), PD-L1 expression (cyan), DAPI for nuclei staining (blue), Scale bar (top left) represents 10 µm. WBCs, white blood cells.

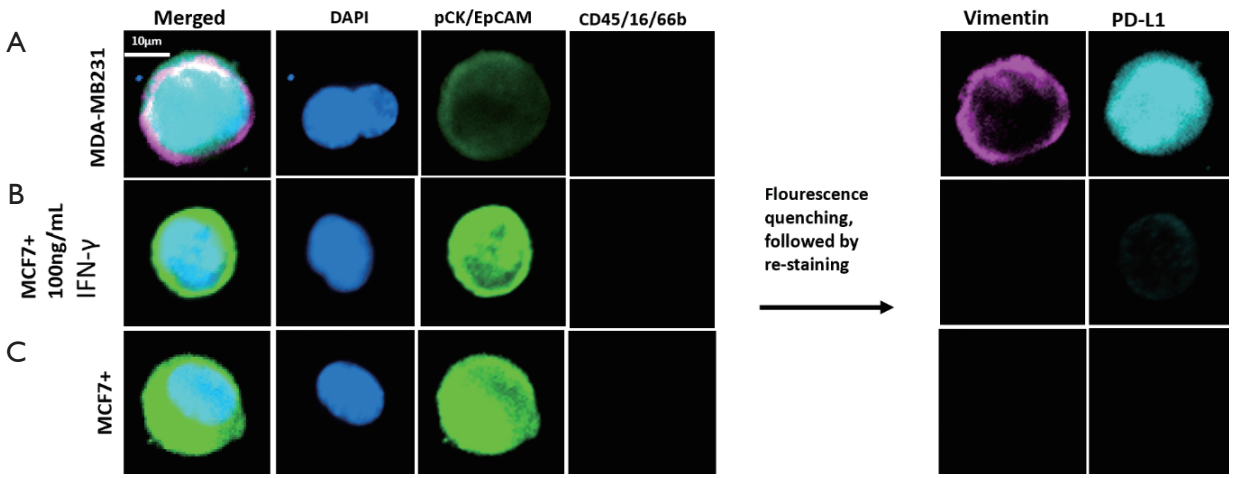

Figure S3 PD-L1 staining controls. Representative images depicting MDA-MB-231 cells (A), IFN-γ induced MCF7 cells (B) and MCF7 cells (C) immune staining with the final carcinoma panel. Cells were stained with FITC/AF488 mixed pan-cytokeratins and EpCAM (green), AF647 CD45, CD16 and CD66b (red), AF647 vimentin (purple) and Cy3 TSA PD-L1 (cyan). Scale bar (top left) represents 10 µm.

https://dx.doi.org/10.21037/tlcr-21-819

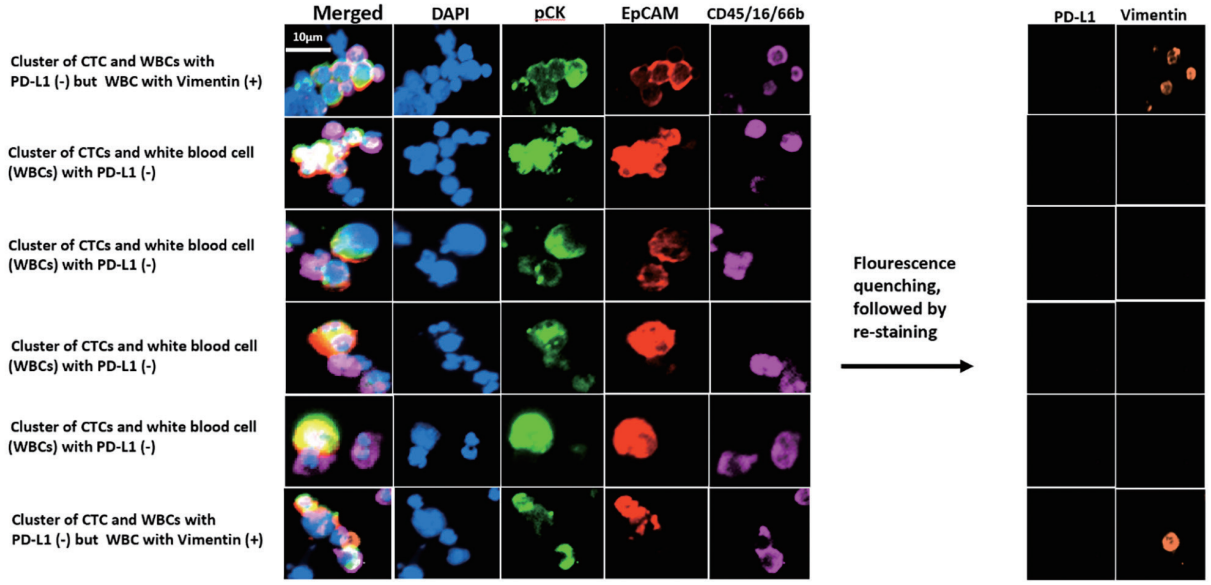

Figure S4 Representative images showing clustered CTC-WBC cells enriched with Parsortix system from SCLC patient blood samples. Cells were stained with FITC/AF488 mixed pan-cytokeratins (green), PE-EpCAM (red), CD45/16/66b AF647 (pink) to identify classical SCLC CTCs, followed by fluorescence quenching and re-immunostained for PD-L1 expression (cyan) and vimentin (orange). Clusters of CTCs and leukocyte, Scale bar (top left) represents 10 μm. CTC, circulating tumour cell; WBCs, white blood cells; SCLC, small-cell lung cancer.

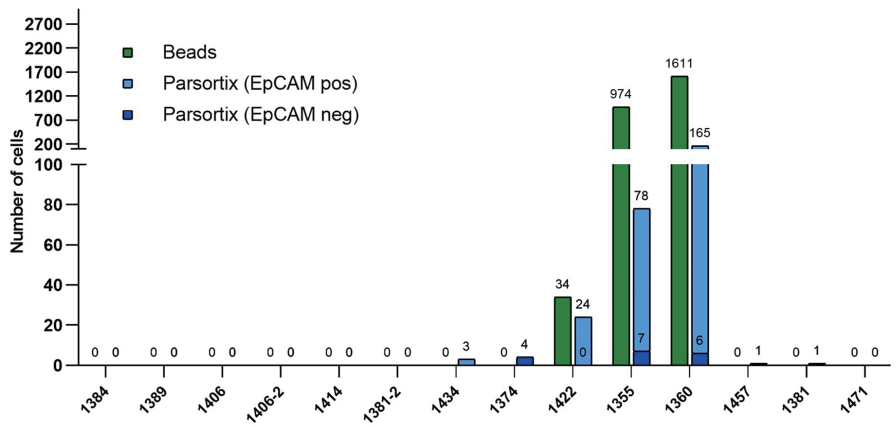

Figure S5 Distribution of EpCAM-positive and negative CTCs enriched by Parsortix. The number of CTCs isolated in matching samples using anti-EpCAM antibody-coated beads were indicated for comparison. CTCs, circulating tumour cells.

https://dx.doi.org/10.21037/tlcr-21-819

Table S2 Association of CTCs thresholds with clinical characteristics (n=21)

Variables	2-CTCs threshold		50-CTCs threshold	
	<2 CTCs (n=9)	≥2 CTCs (n=12)	<50 CTCs (n=15)	≥50 CTCs (n=6)
Age group (years)				
<67	5 (55.6)	4 (33.3)	6 (40.0)	3 (50.0)
≥67	4 (44.4)	5 (66.7)	9 (60.0)	3 (50.0)
P value	0.284		0.523	
Gender				
Female	6 (66.7)	6 (50.0)	6 (40.0)	3 (50.0)
Male	3 (33.3)	6 (50.0)	9 (60.0)	3 (50.0)
P value	0.377		0.523	
Disease Stage				
Limited	2 (22.2)	0 (0.0)	2 (13.3)	0 (0.0)
Extensive	7 (77.8)	12 (100.0)	13 (86.7)	6 (100.0)
P value	0.171		0.500	
Performance status (ECOG)				
0	3 (33.3)	6 (50.0)	7 (46.7)	2 (33.3)
1	3 (33.3)	5 (41.7)	5 (33.3)	3 (50.0)
≥2	3 (33.3)	1 (8.3)	3 (20.0)	4 (16.7)
P value	0.347		0.773	
Number of metastasis				
1	3 (33.3)	2 (16.7)	4 (26.7)	1 (16.7)
≥2	6 (66.7)	10 (83.3)	11 (73.3)	5 (83.3)
P value	0.353		0.550	
Type of treatment				
Chemotherapy	2 (22.2)	5 (41.7)	4 (26.7)	3 (50.0)
Chemotherapy + ICI	6 (66.7)	7 (58.3)	10 (66.7)	3 (50.0)
Radiation	1 (11.1)	0 (0.0)	1 (6.7)	0 (0.0)
P value	0.373		0.524	

CTCs, circulating tumour cells; ECOG, Eastern Cooperative Oncology Group; ICI, immune checkpoint inhibitor.

https://dx.doi.org/10.21037/tlcr-21-819

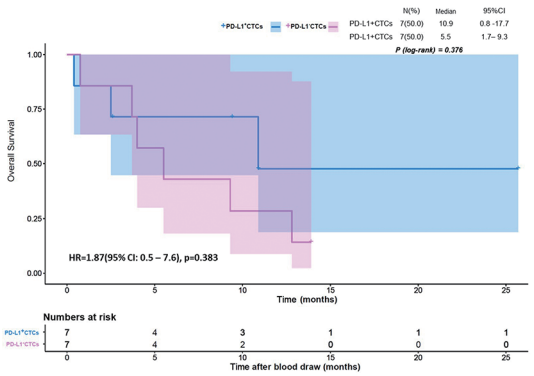

Figure S6 Kaplan-Meier OS curves based on PD-L1 expression on CTCs among SCLC patients. CTCs, circulating tumour cells; CI, confidence interval; HR, hazard ratio; OS, overall survival; SCLC, small-cell lung cancer.

https://dx.doi.org/10.21037/tlcr-21-819